Theoretical analysis of 1.55-µm InAs/InP (113B) quantum dot lasers based on a multi-population rate equation model

F. Grillot*[a,b], K. Veselinov[b], M. Gioannini[c], R. Piron[b], E. Homeyer[b], J. Even[b], S. Loualiche[b] and I. Montrosset[c]

[a]Center for High Technology Materials, The University of New-Mexico, 1313 Goddard SE, 87106 Albuquerque, USA
[b]CNRS-FOTON, 20 Avenue des Buttes de Coësmes, 35043 RENNES Cedex, France
[c]Dipartamento di Elettronica, Politecnico di Torino, Corso Duca degli Abruzzi, 24, Torino, Italy

*fgrillot@chtm.unm.edu

ABSTRACT

Quantum dot (QD) lasers exhibit many useful properties such as low threshold current, temperature and feedback insensitivity, chirpless behavior, and low linewidth enhancement factor. The aim of this paper is to investigate the lasing spectra behaviour of InAs/InP(311B) QD lasers. In order to reach the standards of long-haul transmissions, 1.55-µm InAs QD lasers grown on InP substrate have been developed. More particularly, it has been demonstrated that the use of the specific InP(113)B substrate orientation when combined with optimized growth techniques allows the growth of very small (4 nm high) and dense (up to 10^{11}cm^{-2}) QD structures. Consequently, a model based on the multi-population rate equations (MPRE) taking into account many cavity longitudinal modes for the calculation of the entire emission spectrum has been developed. In order to include the inhomogeneous gain broadening of the QD ensemble, various dot populations, each characterized by a ground state (GS) and an excited state (ES) average energy level have been considered. It will be shown that the numerical results are in good agreement with the experimental ones, both for the case of the double laser emission and for the effects of the homogeneous broadening on the lasing spectra. This numerical investigation based on carrier dynamics is of prime importance for the optimization of low cost sources for optical telecommunications as well as for a further improvement of QD laser performances at 1.55-µm on InP substrate, as already demonstrated for InAs–GaAs QD lasers emitting at 1.3-µm.

Keywords: semiconductor lasers, quantum dots, rate equations.

1. INTRODUCTION

Low-cost, directly modulated lasers will play a major role in the next generation telecommunication links (Local and Metropolitan Area Network) for uncooled and isolator-free applications. As a consequence, semiconductor lasers based on low dimensional heterostructures such as QD laser are very promising. Indeed, QD structures have attracted a lot of attention in the last decade since they exhibit many interesting and useful properties such as low threshold current [1], temperature insensitivity [2], chirpless behavior [3] and optical feedback resistance [4]. Thus, thanks to QD lasers, several steps toward cost reduction can be reached as improving the laser resistance to temperature fluctuation in order to remove temperature control elements (Peltier cooler), or designing feedback resistant laser for isolator-free transmissions and optics-free module. Most investigations reported in the literature deal with InGaAs QD grown on GaAs substrates [5][6]. However, it is important to stress that InGaAs/GaAs QD devices do not usually lead to a laser emission above 1.45-µm [7], which is detrimental for long-haul optical transmission. In order to reach the standards of long-haul transmissions, 1.55-µm InAs QD lasers grown on InP substrate have been developed. More particularly, it has been demonstrated that the use of the specific InP(113)B substrate orientation when combined with optimized growth techniques leads to very small (4-nm high) and dense (up to 10^{11}cm^{-2}) QD structures [8]. Recent experimental studies conducted on these devices have shown that a second laser peak occurs in the laser spectrum when increasing the injection power. This double laser emission is a common property found independently by different research groups both for InGaAs/GaAs and for InAs/InP systems [9][10]. The experimental results in [11] have even shown a saturation and

complete rollover of the first emission after the occurrence of the excited state threshold, while an increasing behavior for both lasing wavelengths has been observed for an InAs/InP(113)B QD laser [9]. The origin of the double emission has been explained by the finite ground state (GS) relaxation time using a cascade relaxation model which brings the GS emission to a constant value after the excited state (ES) threshold [12]. This approach has been also used to extract the dynamical properties of a QD laser [13], while the complete rollover has been attributed to an asymmetry in the thermal population redistribution [14]. A comparison between numerical results and experimental ones has recently been conducted by using either a cascade or a direct relaxation channel model [15]. Such a study has led to demonstrate that when a direct relaxation channel from the wetting layer to the GS is taken into account, the numerical results match very well the measurements and lead to a qualitative understanding of InAs/InP(113)B QD lasers. If no direct relaxation channel is assumed, a good agreement with the experimental results observed in the InAs/GaAs system is obtained.

The aim of this article is to investigate the lasing spectra behavior of 1.55-μm InAs/InP(113B) QD lasers. As a result, a model based on multi-population rate equations (MPRE) is used. The paper is organized as follows: in section 2 a description of the MPRE model is proposed. In order to take into account the inhomogeneous gain broadening of the QD ensemble, the various dot populations, each characterized by a ground state (GS) and an excited state (ES) average energy level have to be considered as in [13]. Then, in section 3, numerical results are presented and compared to experimental ones. The modal gain is at first calculated both for the GS and the ES. When increasing pumping level, numerical results show that the device can emit on the GS only, on the two states or on the ES only. Optical spectra are then calculated considering a laser diode composed of an active region with two InAs QD layers. The transition from the GS to the ES is analyzed with respect to the laser cavity length. The calculated spectra are compared to experimental ones and found to be in good agreement each other. Also the effect of the homogeneous broadening on the lasing spectra characteristics is investigated. For instance, it is demonstrated that due to the direct channel from the WL to the GS, the GS emission continues to grow (even if the ES starts lasing) without a significant broadening of the GS line. Finally, we summarize our results and conclusions in section 4. This numerical model based on a MPRE system is a powerful tool for the prediction of QD devices. Especially, taking into account a direct relaxation channel from the WL to the GS, this opens the way of predicting the behavior of InAs/InP(113B) QD lasers emitting at 1.55-μm. Good agreements with the experimental results, both for the case of the double laser emission as well as for the GS-lasing wavelength shift are demonstrated. This numerical investigation based on carrier dynamics is of prime importance for the optimization of low cost sources for optical telecommunications as well as for a further improvement of QD laser performances at 1.55-μm on InP substrate, as already demonstrated for InAs–GaAs QDs at 1.3-μm [16][17].

2. MULTI-POPULATION RATE EQUATIONS MODEL

In the following, a numerical model is used to study carrier dynamics in the two lowest energy levels of an InAs/InP(113)B QD system. Its active region consists of a QD ensemble with different dots interconnected with the wetting layer (WL). For simplicity the existence of higher excited states is neglected and a common carrier reservoir is associated to both the WL and the barrier. In order to include the inhomogeneous broadening of the gain due the dot size fluctuation the QD ensemble has been divided in n sub-groups each characterized by an average energy of the ES, E_{ESn}, and of the GS, E_{GSn}. The QD are assumed to be always neutral and electrons and holes are treated as eh-pairs and thermal effects and carrier losses in the barrier region are not taken into account. Fig. 1(a) shows a schematic representation of the carrier dynamics in the conduction band for different QD sub-groups in the active region while fig. 1(b) gives more details on the different relaxation mechanisms in the *n-th* QD sub-group. First, an external carrier injection fills directly the WL reservoir with I being the injected current. Some of the eh-pairs are then captured on the fourfold degenerate ES of the QD ensemble with a capture time τ_{ESn}^{WL}. Once on the ES, carriers can relax on the twofold GS τ_{GSn}^{ES}, be thermally reemitted in the WL reservoir τ_{WLn}^{ES} or recombine spontaneously with a spontaneous emission time τ_{ES}^{spon} or by stimulated emission of photons with ES resonance energy. The same dynamic behaviour is followed for the carrier population on the GS level with regard to the ES. This approach has been previously developed for the InAs/GaAs system [11] but in the case of InAs/InP(113)B system it is assumed that at low injection rates, the relaxation processes are phonon-assisted while the Auger effect dominates when the injection gets larger [18]. In order to include this effect, a modified model has been considered introducing a direct relaxation channel τ_{GSn}^{WL} to the standard cascade relaxation model as shown in Fig. 1(b) (dashed line). It is attributed to a single Auger process involving a WL electron captured directly into the GS by transferring its energy to a second WL electron [19]. Carriers are either captured from the WL reservoir into the ES or directly into the GS within the same time $\tau_{GSn}^{WL} = \tau_{ESn}^{WL}$.
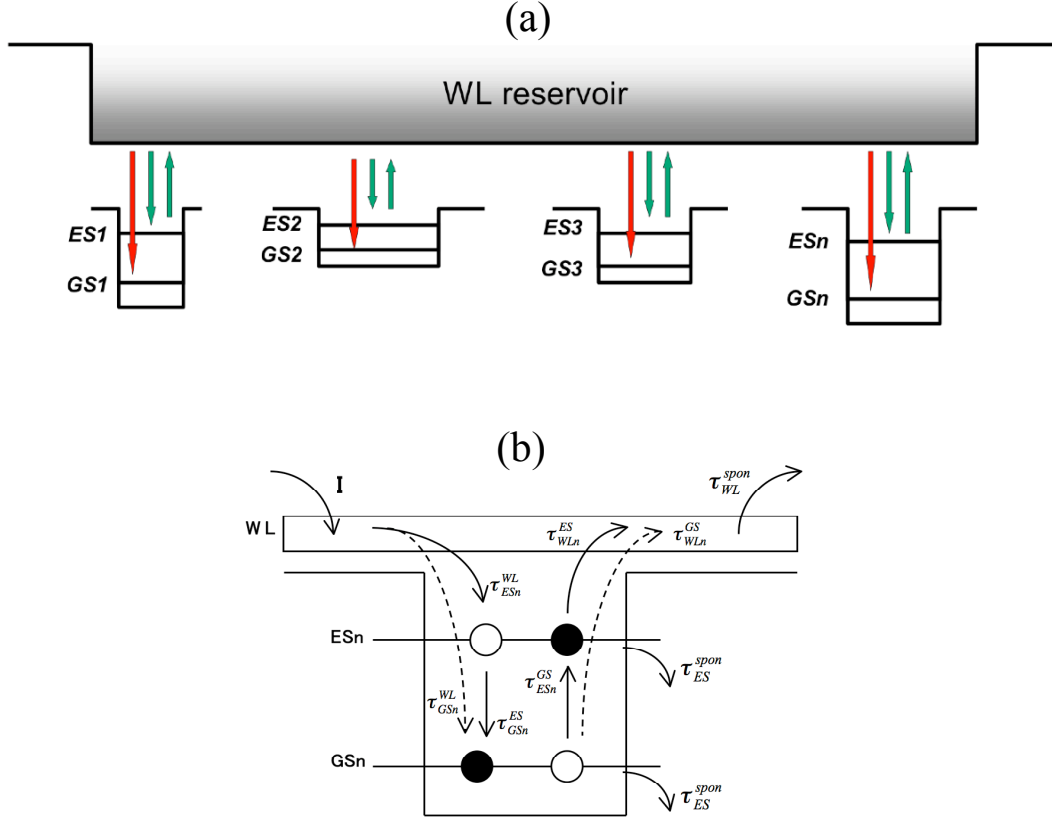
Fig. 1: Schematic representations of the carrier dynamics model with direct relaxation channel for different QD sub-groups in the active region (a) and for the *n-th* QD sub-group (b).

This assumption has been made after analysis of the kinetic curves in [18] where the ES and GS populations gave raise simultaneously 10-ps after excitation. On the other hand carriers can also relax from the ES to the GS. The other transition mechanisms remain the same as in the cascade model. The capture and the relaxation times are then calculated through a phenomenological relation depending on the carrier density in the WL reservoir [20], the ES and GS occupation probabilities and the existence probability of the ES and GS transitions:

$$\tau_{ESn}^{WL} = \frac{1}{\left(A_W + \frac{C_W N_{WL}}{V_{WL}}\right)(1 - P_{ESn})G_{nES}} \tag{1}$$

$$\tau_{GSn}^{ES} = \frac{1}{\left(A_E + \frac{C_E N_{WL}}{V_{WL}}\right)(1 - P_{GSn})} \tag{2}$$

$$\tau_{GSn}^{WL} = \frac{1}{\left(A_W + \dfrac{C_W N_{WL}}{V_{WL}} \right)(1 - P_{GSn}) G_{nGS}}$$ (3)

where N_{WL} is the carrier number in the WL reservoir, V_{WL} is the WL volume and A_W (A_E), C_W (C_E) are the coefficients for phonon and Auger-assisted relaxation respectively, related to the WL and the ES.

P_{ESn} and P_{GSn} are the filling probabilities of the ES and GS respectively in the *n-th* sub-group of dots given by:

$$P_{ESn,GSn} = \frac{N_{ESn,GSn}}{\mu_{ES,GS} N_d w L_{ca} N_l G_{nES,nGS}}$$ (4)

with $N_{ESn,GSn}$ being the ES and GS carrier number in the *n-th* sub-group, $\mu_{ES,GS}$ the degeneracy of the considered confined states, N_d the QD surface density, w and L_{ca} the width and length of the active region and N_l being the number of QD layers. G_{nES} and G_{nGS} are the probabilities of recombination with E_{ESn}, and E_{GSn} energy, respectively. To calculate them, a Gaussian QD size distribution has been considered with a consequent Gaussian distribution of the QD recombination energies. The eh-pairs escape times have been derived considering a Fermi distribution for the ES and GS carriers for the system in quasi-thermal equilibrium without external excitation [12]. To ensure this, the carrier escape time is related to the carrier capture time as follows:

$$\tau_{ESn}^{GS} = \tau_{GSn}^{ES} \frac{\mu_{GS}}{\mu_{ES}} e^{\frac{E_{ESn} - E_{GSn}}{k_B T}}$$ (5)

$$\tau_{WLn}^{ES} = \tau_{ESn}^{WL} \frac{\mu_{ES} N_d N_l}{\rho_{WLeff}} e^{\frac{E_{WL} - E_{ESn}}{k_B T}}$$ (6)

$$\tau_{WLn}^{GS} = \tau_{GSn}^{WL} \frac{\mu_{GS} N_d N_l}{\rho_{WLeff}} e^{\frac{E_{WL} - E_{GSn}}{k_B T}}$$ (7)

where ρ_{WLeff} is the effective density of states in the WL and E_{WL} is its emission energy. The numerical model is based on the MPRE analysis already reported in [13]. According to all those assumptions the MPRE system, describing the change in carrier number of the three electronic energy levels, can be written as:

$$\frac{dN_{WL}}{dt} = \frac{I}{e} + \sum_n \frac{N_{ESn}}{\tau_{WLn}^{ES}} + \sum_n \frac{N_{GSn}}{\tau_{WLn}^{GS}} - \frac{N_{WL}}{\tau_{ES}^{WL}} - \frac{N_{WL}}{\tau_{WL}^{spon}} - \frac{N_{WL}}{\tau_{GS}^{WL}}$$ (8)

$$n = 0, 1, ..., N - 1$$

$$\frac{dN_{ESn}}{dt} = \frac{N_{WL}}{\tau_{ESn}^{WL}} + \frac{N_{GSn}(1 - P_{ESn})}{\tau_{ESn}^{GS}} - \frac{N_{ESn}}{\tau_{WLn}^{ES}} - \frac{N_{ESn}}{\tau_{GSn}^{ES}} - \frac{N_{ES}}{\tau_{ES}^{spon}} - \frac{c\Gamma}{n_r} \sum_m g_{mnES} S_m$$ (9)

$$m = 0, 1, ..., M - 1$$

$$\frac{dN_{GSn}}{dt} = \frac{N_{ESn}}{\tau_{GSn}^{ES}} + \frac{N_{WL}}{\tau_{GSn}^{WL}} - \frac{N_{GSn}(1 - P_{ESn})}{\tau_{ESn}^{GS}} - \frac{N_{GSn}}{\tau_{WLn}^{GS}} - \frac{N_{GS}}{\tau_{GS}^{spon}} - \frac{c\Gamma}{n_r} \sum_m g_{mnGS} S_m$$ (10)

$$m = 0, 1, ..., M - 1$$

with N_{WL} being the carrier number in the wetting layer and Γ the optical confinement factor. In order to calculate the entire emission spectrum, the model has been extended considering also the presence of many cavity longitudinal modes, hence the photon number with resonant energy of the *m-th* mode is depicted by S_m:

$$\frac{dS_m}{dt} = \frac{c\Gamma}{n_r} \sum_n \left(g_{mnES} + g_{mnGS}\right)S_m - \frac{S_m}{\tau_p} + \beta \sum_m \left(B_{ES}\left(E_m - E_{ESn}\right)\frac{N_{ES}}{\tau_{ES}^{spon}} + B_{GS}\left(E_m - E_{GSn}\right)\frac{N_{GS}}{\tau_{GS}^{spon}}\right)\Delta E_m \tag{11}$$

The rate of photons emitted out of the cavity is S_m/τ_p, with τ_p being the photon lifetime. The contribution of the spontaneous emission to the lasing mode is calculated as the sum of the ES and GS spontaneous transitions multiplied by the spontaneous emission coupling factor β, assumed to be constant. In equations (9), (10) and (11) the material gain is described by the set of equations:

$$g_{mnES} = \mu_{ES} \frac{\pi e^2 \hbar}{c n_r \varepsilon_0 m_0^2} \frac{N_d}{H} \frac{\left|P_{ES}^\sigma\right|^2}{E_{ESn}} \left(2P_{ESn} - 1\right)G_{nES}B_{ES}\left(E_m - E_{ESn}\right) \tag{12}$$

$$g_{mnGS} = \mu_{GS} \frac{\pi e^2 \hbar}{c n_r \varepsilon_0 m_0^2} \frac{N_d}{H} \frac{\left|P_{GS}^\sigma\right|^2}{E_{GSn}} \left(2P_{GSn} - 1\right)G_{nGS}B_{GS}\left(E_m - E_{GSn}\right) \tag{13}$$

Here H is the average height of the QD and $\left|P_{ES,GS}^\sigma\right|^2$ is the density matrix momentum [21]. Furthermore let us emphasize that the various QD populations are coupled by the homogenous broadening of the stimulated emission process assumed to be Lorentzian such as:

$$B_{ES,GS}\left(E_m - E_{ESn,GSn}\right) = \frac{\Gamma_{hom}/2\pi}{\left(E_m - E_{ESn,GSn}\right)^2 + \left(\Gamma_{hom}/2\right)^2} \tag{14}$$

with Γ_{hom} being the FWHM of the homogeneous broadening and E_m being the mode energy. All parameters used in the calculations are summarized in Table. 1.

Table 1. Parameters of the QD material and laser

QD material parameters	Laser parameters
Emission energy of the WL, $E_{WL} = 1.05$ eV	Average QD radius, $R = 1.55 \cdot 10^{-6}$ cm
Spontaneous emission from WL, $\tau_{WL}^{spon} = 500\,ps$	Average QD height, $H = 2 \cdot 10^{-7}$ cm
Spontaneous emission from ES, $\tau_{ES}^{spon} = 500\,ps$	Optical confinement factor for the QD, $\Gamma = 0.036$
Spontaneous emission from GS, $\tau_{GS}^{spon} = 1200\,ps$	Mirror reflectivity, $R_1 = R_2 = 0.33$
WL phonon assisted relaxation, $A_W = 1.35 \cdot 10^{10}$ s^{-1}	Cavity internal losses, $\alpha_i = 10$ cm^{-1}
ES phonon assisted relaxation, $A_E = 1.5 \cdot 10^{10}$ s^{-1}	
WL Auger coefficient, $C_W = 5 \cdot 10^{-15}$ m^{3}s^{-1}	
ES Auger coefficient, $C_E = 9 \cdot 10^{-14}$ m^{3}s^{-1}	

In what follows, the MPREM is applied to model the behaviour of InAs/InP(113B) QD laser emitting at 1.55-μm. More particularly, a spectral analysis exhibiting properties linked to the two-sate lasing, the temperature dependence as well as the effects of the cavity length on the emission of properties is investigated both theoretically and experimentally.

3. NUMERICAL RESULTS AND DISCUSSION

1.1 Determination of the modal gain

Applying the MPRE model, the modal gain for a 1-mm long laser with as cleaved facets is calculated and depicted in Fig. 2(a). The level of total loss, which, is represented by the horizontal line, equals ~21-cm^{-1} (assuming internal loss of 10-cm^{-1} which is a typical value on InP substrates). The simulations in fig. 2(a) are performed for different levels of the injected current densities i.e 0, 4, 6, 12, 30, 60 and 300-A/cm^2. The level of loss, which, is represented by the horizontal line, equals 20-cm^{-1} (assuming internal loss of 10-cm^{-1} which is a typical value on InP substrates). Simulations illustrate that when the pumping level goes beyond 6-A/cm^2, the material does not absorb and gain regime occurs for the range of energy under study. When increasing the injected current, a broadening of the gain spectrum is predicted associated to a blue-shit towards higher energy levels (shorter wavelengths). Fig. 2(b) shows the maximum modal gain due to carriers in the GS (solid line) and in the ES (dashed line) as a function of the current density. These simulations show that when the injected current is about ~20-A/cm^2 gain equals loss in the cavity and the GS starts lasing. Then, as far as the injected current increases the GS modal gain saturates at 22.5-cm^{-1}. When the injected current density is increased the gain of the ES equals loss of the cavity: under this situation both the ES and the GS states coexist in the laser structure. This is the situation where the so-called double laser emission is observed. Finally, when the current density gets higher, the ES emission becomes more important and the GS one saturated. As previously mentioned recent experimental studies conducted on QD lasers have shown that a second laser peak appears in the laser spectrum for InAs/GaAs and for InAs/InP systems [9][10].

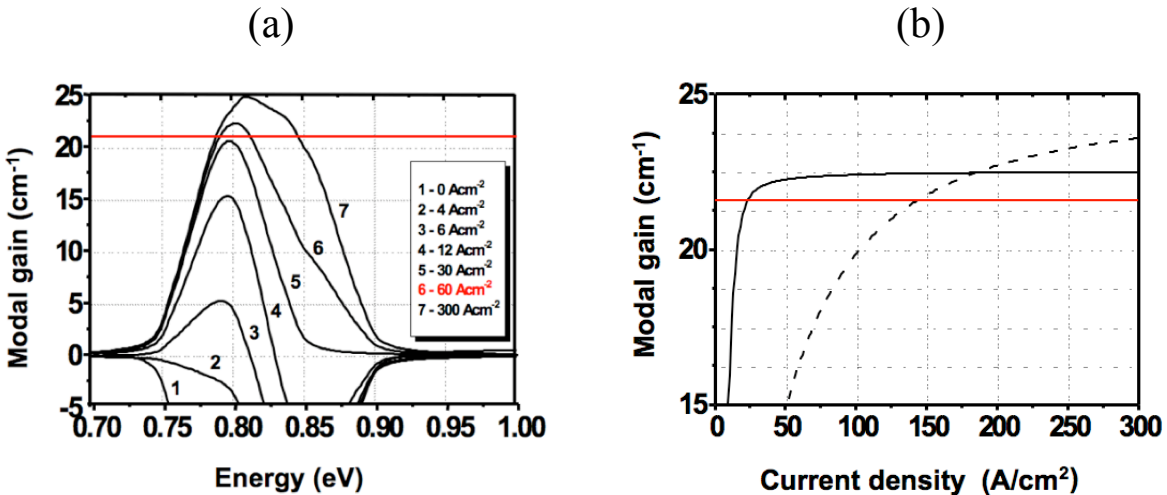(a)   (b)

Fig. 2: The modal gain as a function of energy for different pump currents (a) and the modal gain as a function of the current density for the GS (dotted line) and the ES (dashed line) respectively (b).

More particularly, in the case of the QD lasers grown on InP substrates, it is has been shown in reference [15] that when a direct relaxation channel from the WL to the GS is taken into account, the impact of the double laser emission on the light current characteristic can be properly explained. For instance, [15] shows that in GaAs-based lasers, the emission of the GS saturates completely while the ES emission increases linearly. On the other hand, in the case of InP(113)B devices, the relaxation channel from the WL to the GS induces a slight decrease of the GS slope efficiency (but no saturation) while the global slope efficiency increases. As an example, fig. 3 shows the calculated spectra at room

temperature (RT) of a laser diode composed of an active region with six InAs QD stacked layers. The cavity length is 2.45-mm with cleaved uncoated facets while the width of the strip is 120-µm. In the calculations the homogenous broadening has been fixed to 10-meV. As it can be seen, the GS laser emission is predicted at 0.82-eV (1.51-µm) for $1.04P_{th}$, P_{th} being the threshold pumping power. With increasing pumping power density the emission intensity increases. Then a second stimulated emission appears for 2.08 P_{th} with a laser peak centred at 0.86-eV (1.44-µm). It is worth noting that these numerical results exhibit a very good agreement with experimental ones published in reference [9].
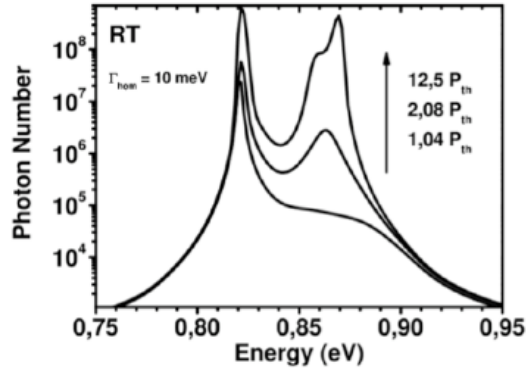

Fig. 3: calculated optical spectrum at room temperature

1. 2 Effect of the cavity length

In order to analyze the effects of the cavity length on the spectrum characteristics, let us now consider the case of a laser diode composed of an active region with two InAs QD layers. The laser structure consists of a waveguide structure comprising 150-nm lattice-matched GaInAsP with a band gap emission wavelength of 1.18-µm (Q1.18) on both sides of the single layer of InAs QDs, self assembled through the Stranski-Krastanov growth mode. Conventional edge-emitting laser with a 100-µm wide ridge structure was formed by wet chemical etching. Long lasers with uncoated as-cleaved facets with an approximate reflectivity of 33% on both sides have been fabricated. In fig. 4, measured spectra are depicted for two cavity lengths: 3-mm (a) and 1-mm (b). These measurements show that for the longer device, the emitting wavelength is centered at ~1.54-µm, which is the signature of the GS-emission. However, when the cavity length goes down to 1-mm, the lasing takes place only from ES transition at ~1.49-µm. It is however important to stress that despite the main contribution in the lasing wavelength comes from the ES, the smaller dots also contribute with their GS at the lasing wavelength. Compare to fig. 2(b) on which a GS lasing emission is predicted for the same cavity length and for a pump current as low as 20A/cm^2, fig. 4(b) shows a direct emission on the ES. This difference can be attributed to a higher loss level. It has been recently shown that the internal loss on InP can range from 10cm^{-1} to 19 cm^{-1} [22]. Consequently, when considering internal loss of 12cm^{-1} (instead of 10cm^{-1}) no GS emission occurs in fig. 2(b) and the laser emits directly on the ES as shown in fig. 4(b). Also in fig. 4, it is shown that a higher threshold current density is required (~700-A/cm^2) for the shorter device emitting on the ES that the one emitting on the GS (~300-A/cm^2). This effect can be attributed to the higher number of eh-pairs needed to obtain transparency in the ES than on the GS due to the degeneracy difference. In Fig. 5, calculated spectra corresponding to the measured results of fig. 4 are depicted. The internal loss value has been adjusted to match the experimental observations in fig. 4(b). As it can be seen a very good agreement between simulations and measurements is obtained. The simulation well reproduces the influence of the cavity length on the lasing wavelength. It is important to stress that the calculated current densities are in a slight disagreement with those depicted in fig. 4. For instance, the current density is about 750-A/cm^2 in fig. 4(b) instead of ~300-A/cm^2 for the calculations in fig. 5(b). We believe such a difference may come from leakage currents, which are not included in the model meaning that values of current densities are probably underestimated in the calculations. When longer cavity lengths are considered, the lasing wavelength remains relatively constant located at the GS transition around 1.54-µm (see fig. 5(a)). Then, when decreasing the cavity length below 2-mm, the lasing wavelength slightly shifts down to 1.49-µm (see fig. 5(b)) which corresponds to the 1-mm long cavity. Such a transition from the GS to the ES shows that the GS always contributes to lasing emission but its contribution decreases as long as the lasing wavelength moves from longer to shorter wavelength.
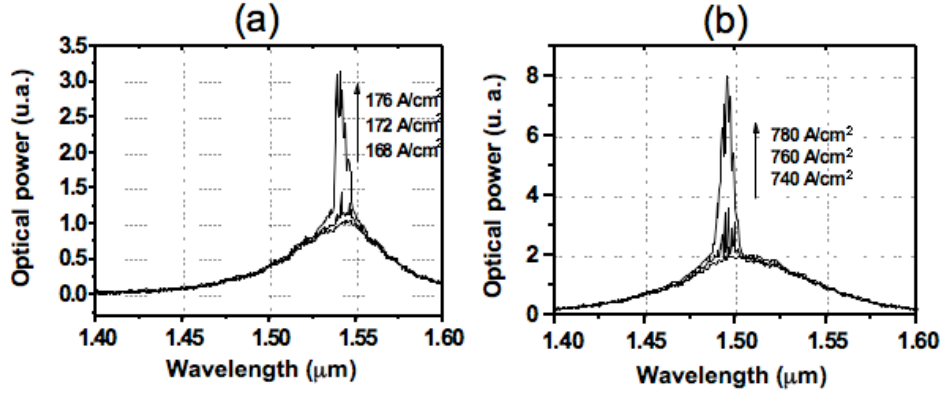
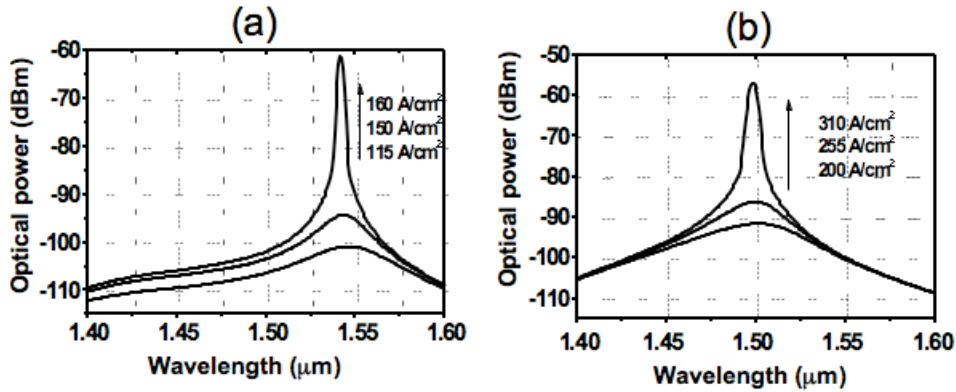Fig. 4: Measured spectra for two cavity lengths (a) 3mm and (b) 1mm

Fig. 5: Calculated spectra for two cavity lengths (a) 3mm and (b) 1mm

1.3 Effect of the temperature on the lasing characteristics

In order to analyze the effects of the temperature on the spectrum characteristics let us consider a laser diode composed of an active region with one InAs QD layer [23]. A 5mm long laser with uncoated as-cleaved facets with an approximate reflectivity of 33% on both sides was fabricated. In Fig. 6, lasing and electroluminescence spectra under pulsed electrical injection are shown for two different temperatures: 110K (a) and 253K (b). At each temperature, spectra at several injections current are displayed and the threshold current (I_{th}) is given. As it can be seen, a drastic narrowing of the electroluminescence spectra is observed with increasing temperature. Thus, at low temperature (110K), a very broad-band multimode lasing spectra up to 26meV width (50nm) at high injection current (500mA) is observed. The laser emission progressively narrows with rising temperature, leading to spectra with a width of 2.8meV (6nm) at 253K and for an injected current of 880mA. The observed temperature dependence of lasing spectra can be explained qualitatively by taking into account the homogeneous broadening of the optical gain of a single dot. At low temperature, when the homogeneous broadening is negligible, dots with different energies have a relatively narrow individual optical gain (narrow single dot linewidth with a FWHM below 2nm [21] and since they are spatially isolated from each other, there is no correlation between the individual emissions. Then, all dots that have an optical gain above the lasing threshold start lasing independently, leading to broad-band lasing emission. On the other hand, when homogeneous broadening is comparable to inhomogeneous broadening, lasing mode photons are emitted not only from energetically resonant dots but also from other non-resonant dots within the range of the homogeneous broadening. This leads to a collective lasing emission with narrow line of a dot ensemble, which explains the emission spectra observed at 253K close to room temperature.
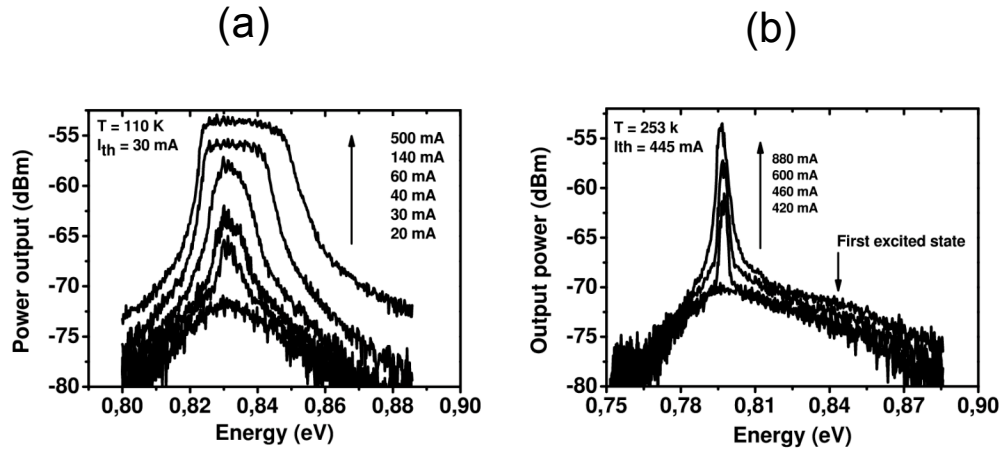
Fig. 6: Lasing and electroluminescence spectra under pulsed injection mode for two different temperatures: (a) 110 K and (b) 253 K. At each temperature, spectra at several injection currents are displayed and the threshold current (I_{th}) is given.

In Fig. 7, calculated spectra corresponding to the laser described above are presented. The first situation is calculated for a temperature equal to 110K while the other one corresponds to a temperature fixed to 253K. In both cases, a very good agreement with experimental results depicted in Fig. 6 is qualitatively observed. At low temperature, the homogeneous broadening is assumed to be equal to 3meV in agreement with [10]. As expected, the lasing spectrum is very broad and that corresponds to nearly individual emission of the dots as it has been experimentally observed at low temperature [23][24]. On the other hand, close to room temperature, when the homogeneous broadening (30meV in the calculations) reaches the same order of magnitude of the inhomogeneous broadening, it connects spatially isolated and energetically different quantum dots, leading to the collective lasing emission. These simulations demonstrate that dots with different energies start lasing independently at low temperature while at higher ones dots contribute to lasing collectively via homogeneous broadening of optical gain
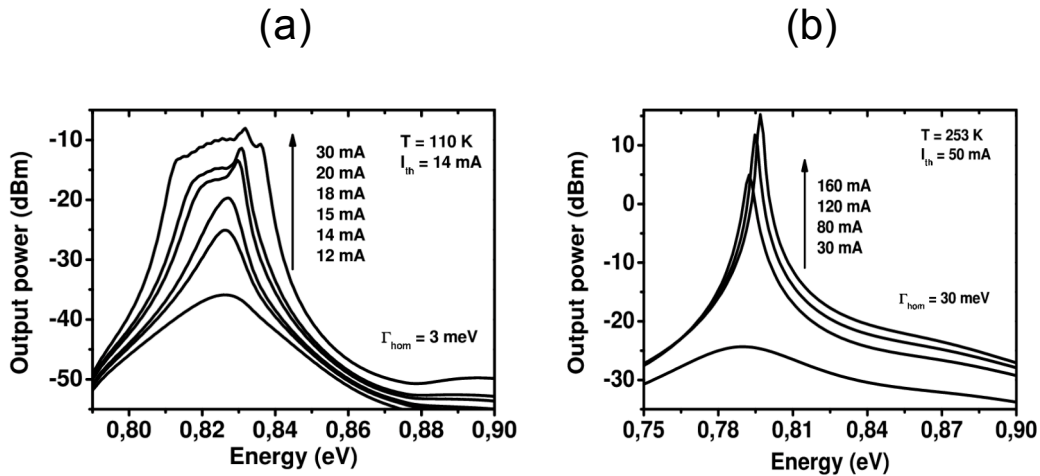

Fig. 7: Calculated emission spectra of a semiconductor laser with a single QD layer on InP(113)B substrate for two different temperatures: (a) 110 K and (b) 253 K.

IV. CONCLUSIONS

In this paper, a theoretical model has been used to investigate the lasing spectrum properties of InAs/InP(113)B QD lasers emitting at 1.55-µm. The numerical model is based on a MPRE analysis and takes into account the QD size dispersion as well as the temperature dependence through both the inhomogeneous and the homogenous broadenings. Especially this article has highlighted the influence of the cavity length on the lasing wavelength as well as the effects of the temperature through the homogenous broadening. Consequently, optical spectra have been calculated for different cavity loss levels. Simulations have demonstrated in agreement with the experiments that the gain peak switches from the GS to the ES energy when current density is increased. Then, the temperature dependence of lasing spectra has been studied both experimentally and theoretically. It has been shown that dots with different energies start lasing independently at low temperature due to their spatial localization while at room temperature the dot ensemble contributes to a narrow line lasing collectively via the homogeneous broadening of optical gain. As a conclusion, this numerical tool opens the way of predicting the behavior of InAs/InP(113B) QD lasers emitting at 1.55-µm which have recently shown improved performances [25]. This numerical investigation based on carrier dynamics is of prime importance for the optimization of low cost sources for optical telecommunications as well as for a further improvement of QD laser performances at 1.55-µm on InP substrate.

REFERENCES

[1] Liu, G. T., Stintz, A., Li, H., Malloy, K. J. and Lester, L. F., "Extremely low room-temperature threshold current density diode lasers using InAs dots in In $_{0.15}$Ga$_{0.85}$ As quantum well", Electron. Lett., 35(14), 1163-1165(1999).

[2] Mikhrin, S. S., Kovsh, A. R., Krestnikov, I. L., Kozhukhov, A. V., Livshits, D. A., Ledentsov, N. N, Shernyakov, Y. M., Novikov, I. I, Maximov, M. V., Ustinov, V. M. and Alferov, Zh. I., "High power temperature-insensitive 1.3µm InAs/InGaAs/GaAs quantum dot lasers", Semicond. Sci. Technol., 20, 340-342(2005).

[3] Saito, H., Nishi, K., Kamei, A. and Sugou, S., "Low chirp observed in directly modulated quantum dot lasers", IEEE Photon. Technol. Lett. 12(10), 1298-1300(2000).

[4] O'Brien, D., Hegarty, S. P., Huyet, G., McInerney, J. G., Kettler, T., Laemmlin, M., Bimberg, D., Ustinov, V. M., Zhukov, A. E., Mikhrin, S. S., Kovsh, A. R., "Feedback sensitivity of 1.3µm InAs/GaAs quantum dot lasers" Electron. Lett., 39(25), 1819-1820(2003).

[5] Grundmann, M., Stier, O., Bognar, S., Ribbat, C., Heinrichsdorff, F. and Bimberg, D., "Optical Properties of Self-Organized Quantum Dots: Modelling and Experiments", Phys. Stat. Sol., 178(1), 255-262(2000).

[6] Hatori, H., Sugawara, M., Mukai, K., Nakata, Y. and Ishikawa, H., "Room-temperature gain and differential gain characteristics of self-assembled InGaAs/GaAs quantum dots for 1.1-1.3 µm semiconductor laser", App. Phys. Lett., 77, 773-775(2000).

[7] Karachinsky, L. Y., Kettler, T., Gordeev, N. Yu., I. I., Novikov, Maximov, M. V., Shernyakov, Yu. M., Kryzhanovskaya, N. V., Zhukov, A. E., Semenova, E. S., Vasil'ev, A. P., Ustinov, V. M., Ledentsov, N. N., Kovsh, A. R., Shchukin, V. A., Mikhrin, S. S., Lochmann, A., Schulz, O., Reissmann, L. and Bimberg, D., "High-power singlemode CW operation of 1.5 µm range quantum dot GaAs-based laser", Electron. Lett., 41(8), 478-479(2005).

[8] Caroff, P., Paranthoën, C., Platz, C., Dehaese, O., Folliot, H., Bertru, N., Labbé, C., Piron, R., Homeyer, E., Le Corre, A., Loualiche, S., "High gain and low threshold InAs quantum dot lasers on InP", App. Phys. Lett., 87, 243107(2005).

[9] Platz, C., Paranthoen, C., Caroff, P., Bertru, N., Labbe, C., Even, J., Dehaese, O., Folliot, H., Le Corre, A., Loualiche, S., Moreau, G., Simon, J. C. and Ramdane, A., "Comparison of InAs quantum dot lasers emitting at 1.55 µm under optical and electrical injection", Semicond. Sci. Technol., 20, 459-463(2005).

[10] Sugawara, M., Hatori, N., Ebe, H., Arakawa, Y., Akiyama, T., Otsubo, K. and Nakata, Y., "Modelling room-temperature lasing spectra of 1.3 µm self-assembled InAs/GaAs quantum-dot lasers: Homogeneous broadening of optical gain under current injection", Journal of Applied Physics, 97, 043523(2005).

[11] Markus, A., Chen, J. X., Paranthoën, C., Fiore, A., Platz, C. and Gauthier-Lafaye, O., "Simultaneous two-state lasing in quantum-dot lasers", App. Phys. Lett., 82, 1818-1820(2003).

[12] Markus, A., Chen, J. X., Gauthier-Lafaye, O., Provost, J. G., Paranthoën, C. and Fiore, A., "Impact of Intraband

Relaxation on the Performance of a Quantum-Dot Laser", IEEE Journal of Selected Topics in Quantum Electron., 9(5), 1308-1314(2003).

[13] Gioannini, M., Sevega, A. and Montrosset, I., "Simulations of differential gain and linewidth enhancement factor of quantum dot semiconductor lasers", Optical and Quantum electronics, 38(4), 381-394(2006).

[14] Viktorov, E. A., Mandel, P., Tanguy, Y., Houlihan, J. and Huyet, G., "Electron-hole asymmetry and two-state lasing in quantum dot lasers", App. Phys. Lett., 87, 053113(2005).

[15] Veselinov, K., Grillot, F., Cornet, C., Even, J., Bekiarski, A., Gioannini, M. and Loualiche, S., "Analysis of the Double Laser Emission Occurring in 1.55-µm InAs–InP (113)B Quantum-Dot Lasers", IEEE Journal of Quantum Electron., 43(9), 810-816(2007).

[16] Dagens, B., Bertran-Pardo, O., Fischer, M., Gerschutz, F., Koeth, J., Krestnikov, I., Kovsh, A., Le Gouezigou, O., Make, D., "Uncooled Directly Modulated Quantum Dot Laser 10Gb/s Transmission at 1.3µm with Constant Operation Parameters", Proc. ECOC, Th4.5.7, Post deadline paper(2006.)

[17] Gershutz, F., Fischer, M., Koeth, J., Chacinski, M., Schatz, R., Kjebon, O., Kovsh, A., Krestinkov, I. and Forschel, A., "Temperature insensitive 1.3µm InGaAs/GaAs quantum dot distributed feedback lasers for 10Gbit/s transmission over 21km", Electron. Lett., 42(25), 1457-1458(2006).

[18] Miska, P., Paranthoën, C., Even, J., Dehaese, O., Folliot, H., Bertru, N., Loualiche, S., Senes, M. and Marie, X., "Optical spectroscopy and modelling of double-cap grown InAs/InP quantum dots with long wavelength emission", Semicond. Sci. Technol., 17, 63-67(2002).

[19] Ohnesorge, B., Albrecht, M., Oshinowo, J., Arakawa, Y. and Forchel, A., "Rapid carrier relaxation in self-assembled $In_xGa_{1-x}As$/GaAs quantum dots", Phys. Rev. B, 54(16), 11532-11538(1996).

[20] Berg, T., Bischoff, s., Magnusdottir, I. and Mork, J., "Ultrafast Gain Recovery and Modulation Limitations in Self-Assembled Quantum-Dot Devices", IEEE Photon. Technol. Lett, 13(6), 541-543(2001).

[21] Sugawara, M., Mukai, K., Nakata, Y. and Ishikawa, H., "Effect of homogeneous broadening of optical gain on lasing spectra in self-assembled $In_xGa_{1-x}As$/GaAs quantum dot lasers", Phys. Rev. B, 61, 7595-7603(2000).

[22] Zhou, D., Piron, R., Grillot, F., Dehaese, O., Homeyer, E., Dontabactouny, M., Batte, T., Tavernier, K., Even, J. and Loualiche, S., "Study of the characteristics of 1.55µm quantum dash/dot semiconductor lasers on InP substrate," Appl. Phys. Lett., 93, 161104 (2008).

[23] Homeyer, E., Piron, R., Caroff, P., Paranthoen, C., Dehaese, O., Le Corre, A. and Loualiche, S., "Temperature studies on a single InAs/InP QD layer laser emitting at 1.55µm", Phys. Stat. Sol. (c), 3(3), 407-410(2006).

[24] Sugawara, M., Mukai, K. and Nakata, Y., "Light emission spectra of columnar-shaped self-assembled InGaAs/GaAs quantum-dot lasers: Effect of homogeneous broadening of the optical gain on lasing characteristics", Appl. Phys. Lett., 74, 1561(1999).

[25] Martinez, A., Merghem, K., Bouchoule, S., Moreau, G., Ramdane, A., Provost, J. G., Alexandre, F., Grillot, F., Dehaese, O., Piron, R. and Loualiche, S., "Dynamic properties of InAs/InP(311B) quantum dot Fabry-Perot lasers emitting at 1.52-µm", Appl. Phys. Lett., 93, 021101(2008).